This is an accepted manuscript of an article published by Elsevier in Blood Cells, Molecules and Diseases (accepted 05/02/2016) available at: doi.org/10.1016/j.bcmd.2016.02.001.

Plasmodium falciparum infection induces dynamic changes in the erythrocyte phospho-proteome

Guillaume Bouyer[1,2], Luc Reininger[3,4], Ghania Ramdani[3,4], Lee Phillips[5], Vikram Sharma[5,6], Stephane Egee[1,2], Gordon Langsley[3,4], Edwin Lasonder[5$]

1 Sorbonne Universités, UPMC Univ Paris 06, UMR 8227, Comparative Physiology of Erythrocytes, Station Biologique de Roscoff, CS 90074, Roscoff, France.

2 Centre National de la Recherche Scientifique, UMR 8227, Comparative Physiology of Erythrocytes, Station Biologique de Roscoff, CS 90074, Roscoff, France.

3 Laboratoire de Biologie Cellulaire Comparative des Apicomplexes, Faculté de Médécine, Université Paris Descartes, 27, rue du Faubourg-Saint-Jacques, 75014 Paris, France

4 Institut Cochin, INSERM U1016, CNRS UMR 8104, Paris, France

5 School of Biomedical and Healthcare Sciences, Plymouth University, Drake Circus, Plymouth, Devon, UK

6 Systems Biology Centre, Plymouth University Peninsula Schools of Medicine and Dentistry, Plymouth University, Drake Circus, Plymouth, Devon, UK

$ corresponding author

Abstract

The phosphorylation status of red blood cell proteins is strongly altered during the infection by the malaria parasite *Plasmodium falciparum*. We identify the key phosphorylation events that occur in the erythrocyte membrane and cytoskeleton during infection, by a comparative analysis of global phospho-proteome screens between infected (obtained at schizont stage) and uninfected RBCs. The meta-analysis of reported mass spectrometry studies revealed a novel compendium of 495 phosphorylation sites in 182 human proteins with regulatory roles in red cell morphology and stability, with about 25% of these sites specific to infected cells. A phosphorylation motif analysis detected 7 unique motifs that were largely mapped to kinase consensus sequences of casein kinase II and of protein kinase A / protein kinase C. This analysis highlighted prominent roles for PKA / PKC involving 78 phosphorylation sites. We then compared the phosphorylation status of PKA (PKC) specific sites in adducin, dematin, Band 3 and GLUT-1 in uninfected RBC stimulated or not by cAMP to their phosphorylation status in iRBC. We showed cAMP-induced phosphorylation of adducin S59 by immunoblotting and we were able to demonstrate parasite-induced phosphorylation for adducin S726, Band 3 and GLUT-1, corroborating the protein phosphorylation status in our erythrocyte phosphorylation site compendium.

Abbreviations:

CK1 and CK2, casein kinases I and II; GO, gene ontology; GLUT-1, glucose transporter 1; iRBC, infected red blood cell; LC-MS/MS, liquid chromatography tandem mass spectrometry; LFQ, label free quantification; PTMs, post-translational modifications; PKA, protein kinase A; PKC, protein kinase C

Keywords: Erythrocyte; *P. falciparum*; Protein phosphorylation; cAMP / protein kinase A; GLUT-1; Cytoskeleton

1.1 Introduction

Mammalian erythrocytes have been widely studied for cytoskeleton structure, membrane composition and transport properties. Over the last decade, numerous studies have incorporated mass spectrometry techniques to mine and quantify the proteins expressed in red blood cells (RBCs) and to link these proteins functionally to various physiological or pathophysiological situations. However, even if these cells have a simple structural organization and specific function, proteomics studies have proven difficult to get a good overview of the diversity of proteins in RBCs for several reasons: (i) the abundance of ultra-majoritarian proteins in the cytosol (haemoglobin, up to 98% of cytosolic proteins at an unrivalled concentration: 5 mM – 340 g/l) and in the membrane (Band 3, 1 M copies/cell) and (ii) the tight links between membrane and sub-membranous cytoskeleton. With the progression of techniques, the number of proteins identified has raised to an unexpected number of 1578 unique proteins in the cytosol [1], and a total number of 2289 unique proteins in the RBC identified so far [2].

The next challenge now is to link these proteins to physiological processes, and one key feature is to elucidate the regulatory role of various post-translational modifications (PTMs). These modifications include oxidation effects, glycosylation, palmitoylation and most of all protein phosphorylation. Indeed, kinase activities have been described as a key regulatory mechanism in RBC and deregulation of their activities seems to be implicated in multiple diseases [3] including malaria, the focus of this study. Human RBCs in circulation harbour various active protein kinases, including protein kinase C (PKC), protein kinase A (PKA), casein kinases I and II (CK1 and CK2), Syk, Lyn, Hck-Fgr, and Fyn, as reviewed by Pantaleo et al. [4]. Activity of these kinases has been mostly studied regarding their effects on cytoskeleton or membrane proteins in various physiological or pathophysiological contexts.

Spectrin phosphorylation by casein kinase has been associated with membrane destabilization [5] and enhanced spectrin phosphorylation is linked to hereditary elliptocytosis and pyropoikilocytosis [6]. The horizontal junctional complex components are also phosphorylated; the combined phosphorylation of adducin and protein 4.1 by PKC decreased their binding to spectrin and actin, resulting in weaker

membrane stability [7]; dematin is known to be phosphorylated by PKA, leading to disruption of actin/spectrin binding [8]. Regarding vertical complexes and integral membrane proteins, Band 3 PTMs have been widely studied (in regard to its pivotal role in membrane transport and structure). Notably, Band 3 tyrosine phosphorylation triggers its dissociation from ankyrin, consequently releasing Band 3 from spectrin/actin cytoskeleton [9].

The present study focusses on the changes in RBC protein phosphorylation resulting from infection with the human malaria causing parasite *Plasmodium falciparum*. During its complex life cycle, the parasite invades RBCs, where it is largely hidden from the host immune system. Inside erythrocytes it multiplies via the process of schizogony every 48 h to form up to 32 new merozoites. After rupture of infected RBCs, merozoites are released to invade fresh red cells and to complete a new cycle of asexual development. During intra-erythrocytic development, the parasite remodels the red blood cell surface, notably by exporting proteins to the host cytosol and membrane and by forming knobs that mediate interactions with host endothelial cells to escape clearance of infected RBCs (iRBC) by the spleen. The process of sequestration and cytoadherence of iRBCs results in clogging of blood vessels in various organs and it contributes to the clinical symptoms of malaria. Host cell permeability [10] or deformability [11] are also largely modified upon infection. Various exported parasite proteins play crucial roles in this process, and lately it''s becoming clear that an involvement of host proteins is also required for parasite-mediated host cell remodelling. Multiple host proteins see their phosphorylation status altered during infection, which was demonstrated by the pioneering study of Wu et al. [12], who in 2009 showed increased phosphorylation during parasite infection by immunoblotting and mass spectrometry. With the emergence of liquid chromatography tandem mass spectrometry, several studies [13—16] followed with phospho-proteome analyses of iRBCs, but remarkably largely ignored published data on phosphorylation sites identified in human red blood cell proteins. This study summarizes our current knowledge on RBC phosphorylation by comparing published phosphorylation sites measured in normal and *P. falciparum* infected RBCs and experimentally validating some of the major findings.

2. Material and methods

2.1. Compendium of red blood cell phosphorylation sites

Phospho-peptide sequences identified in large scale RBC phospho-proteome LC–MS/MS studies with data taken from normal [17] and *P. falciparum*-infected RBCs at the schizont life cycle stage [13–16] were remapped to the UNIPROT protein database using the software tool Protein Coverage Summarizer (http://omics.pnl.gov/software/protein-coverage-summarizer) in order to generate a uniform format for comparing phosphorylation sites across data sets. The compendium of phospho-sites included all sites detected in normal RBCs from Soderblom et al. [17], and sites from infected RBCs that were detected at least twice in the four independent studies [13–16].

2.2. Phosphorylation motif analyses

Phosphorylation sites were categorized by their chemical properties as acidic, basic, proline-directed, tyrosine or other by a decision tree method described previously [14] as follows: 1) get the 6 neighbouring amino acids before and after the phosphorylation site; 2) pY at position 0 then classify as “Tyrosine”; 3) P at+1 then classify as “Proline-directed”; 4) positions +1 to +6 contain more than one D and E residues then classify as “Acidic”; 5) K or R at position −3 then classify as “Basic”; 6) D or E at +1,+2, or +3 then classify as “Acidic”; 7) between −6 and −1 more than 2 K or R residues then classify as “Basic”; 8) remaining peptides classify as “Other”. Phosphorylation motifs were identified using MotifX [18] with the following parameters: phosphorylation motif window = 13 amino acids, p-value threshold = $1 * 10^{-4}$ for S and T residues, $1 * 10^{-3}$ for Y residues, motif fold increase $\geqslant$2, a motif frequency N5, and a background of all RBC proteins identified. The analysis was repeated for a degenerate amino acid set with conservative amino acid substitutions within the motif window according to: A = AG, D = DE, F = FY, K = KR, I = ILVM, Q = QN, S = ST, C = C,H=H, P=P,W=W. When different motifs were found for a peptide by the analyses with different amino acid residues, priority was given to the motif with the highest MotifX score. Sequence logos were generated with Weblogo 3 [19] from http://weblogo.threeplusone.com/create.cgi. The motifs were matched to known

protein kinase target motifs using PhosphoMotifFinder [20] and matches were considered as potential links between phosphorylation motifs and protein kinases.

2.3. Gene ontology (GO) analysis

GO enrichment analyses of lists of membrane-associated phosphoproteins from infected and normal RBCs were carried out using the web tool Database for Annotation Visualization and Integrated Discovery (DAVID, version 6.7. http://david.abcc.ncifcrf.gov/) [21,22] with a background set of all human proteins. Enrichment of GO FAT terms was considered statistically significant when corrected for multiple testing by the Benjamini–Hochberg method with adjusted p-values lower than 0.05. Overlap between enriched GO terms was visualised in a network with the Cytoscape plugin Enrichment Map [23].

2.4. Cell preparation and Western blotting

Human RBCs were drawn from healthy volunteers under informed consent, washed several times in RPMI, kept in culture medium (see below) and used within one week of collection. *P. falciparum* NF54 was grown in RBCs as described previously, using 0.5% Albumax II® (Invitrogen) instead of human serum [52]. Parasites were synchronized twice using 5% w/v sorbitol solution according to Lambros and Vanderberg [53]. Schizont-stage parasite cultures were then enriched to N95% by centrifugation on a 70% Percoll/sorbitol solution as described in [24]. Parasite growth and development of schizont stages was monitored by Giemsa-stained thin blood smears. Uninfected RBC controls were incubated for 48 h in culture medium at 37 °C and kept in the presence or absence of 50 μM dibutyryl-cAMP (Sigma Aldrich), a cell-permeable non-hydrolysable cAMP analogue that activates protein kinase A, for the last 30 min before harvesting. Cell counts were determined by using a Cellometer Mini (Nexcelom Bioscience) automated cell counter following manufacturer's recommendations.

Western blotting of uninfected RBCs and *P. falciparum*-infected RBC (1 × 107) samples was performed using erythrocyte ghosts. Briefly, RPMI-washed erythrocytes were incubated in 20 volumes of ice-cold hypotonic buffer 5P8 (5 mM NaH2PO4, pH 8.0) containing 1 mM phenylmethylsulfonyl fluoride, protease inhibitor mix (1 μg each of chymostatin, leupeptin, antipain, and pepstatin and 8 μg aprotinin

per ml), and phosphatase inhibitors (10 mM Na fluoride, 2mMβ-D glycerophosphate, 1 mM Na orthovanadate), then washed several times in 5P8 containing protease and phosphatase inhibitors (30 min centrifugation 14,000 ×g at 4 °C). Membrane proteins were solubilized in lysis buffer (150 mM NaCl, 10 mM KCl, 1 mM MgCl2, 20mM Tris–HCl pH 7.5, 1% Triton X-100) in the presence of protease and phosphatase inhibitors. *P. falciparum*-infected RBC samples were further lysed by sonication followed by centrifugation at 10,000 ×g. Dephosphorylation of proteins was achieved by incubation with λ-protein phosphatase in 1× NE Buffer (New England BioLabs, Inc.) supplemented with 1 mM MnCl2 for 30 min at 30 °C. A Bradford protein assay kit (Bio-Rad Laboratories) was used to determine protein concentrations. Protein samples diluted in reducing Laemmli buffer were separated using NuPAGE 10% Bis-Tris (Invitrogen) SDS-PAGE. Western blotting was performed using standard methods. Antibodies used to probe RBC membrane antigens were rabbit monoclonal anti-α-adducin phospho Ser59 (Abcam ab76251) 1/500; rabbit polyclonal anti-α-adducin phospho Ser726 (Santa Cruz sc101627) 1/200; mouse monoclonal anti-α-adducin (Abcam ab54985) 1/1000; rabbit polyclonal anti-dematin phospho Ser 403 (Sigma-Aldrich SAB4504167), 1/500; mouse polyclonal anti-dematin (Abcam ab89161) 1/500; horseradish peroxidase-conjugated goat anti-rabbit IgG (H + L)/goat anti-mouse IgG (H + L) (Bio-Rad Laboratories) 1/3000. Pierce ECL 2 Western blotting detection reagent (Thermo Scientific) was used and fluorescent signals were captured by Typhoon fluorescence imager (GE Healthcare Life Sciences).

For immunoprecipitation, uninfected RBCs and *P. falciparum* infected RBC (1×10^8) lysates were incubated with rabbit monoclonal anti-phospho-Akt substrate RxxS*/T* (110B7E) antibody conjugated to sepharose beads (9646 Cell Signalling) for 4 h at 4 °C, then washed 3 times with lysis buffer containing protease and phosphatase inhibitors. Samples were eluted by boiling the beads in reducing Laemmli buffer, then subjected to SDS-PAGE and Western blotting using standard methods. Membranes were probed with mouse monoclonal anti-Band 3 (BIII-136, Sigma B9277) 1/20,000 and mouse monoclonal anti-GLUT-1 (Abcam ab40084) 1/2500.

2.5. Mass spectrometry

Ghost preparations of uninfected RBCs and Percoll-purified schizont stage *P. falciparum*-infected RBCs (N95% enrichment, 100 µg) were digested in solution by trypsin using the FASP procedure [25], and tryptic peptides were purified by STAGE tips [26]. Liquid chromatography tandem mass spectrometry analysis of tryptic peptides (500 ng) was performed on the Orbitrap Velos Pro mass spectrometer (Thermo Fisher, Bremen, Germany) equipped with the Ultimate 3000 UPLC system (Thermo Fisher, Germany) as previously described in [27]. Protein identification at 1% FDR and label free quantification (LFQ) were performed using MaxQuant [28] with settings that were described in [27].

3. Results

3.1. Compendium of protein phosphorylation sites in red blood cells

Changes in phosphorylation events at serine, threonine and tyrosine amino acid residues of human red cell proteins induced by infection with the malaria parasite *P. falciparum* were established by a comparative analysis of the four published phospho-proteomes of parasite-infected cells [13–16] with normal red cells [17]. Large scale *P. falciparum* phospho-proteome studies were primarily focussed at the schizont intra-cellular life cycle stage identifying more than 9000 parasite phosphorylation sites at various confidence levels [29]. We therefore required detection by at least two independent studies for inclusion of human red blood cell phosphorylation sites in this study. The uninfected red cell phosphorylation sites were taken from the work of Soderblom et al. as part of their investigation of the ERK1/2-mediated human phosphorylation changes in sickle red blood cell membrane [17]. Taken together, we generated a novel information source comprising 495 phosphorylation sites in 182 human proteins (Table S1) that combines 380 sites found in normal red cells and 274 sites described for infected red cells with 158 phospho-sites in common, as depicted in the Venn diagram (Fig. 1A). The distribution of phosphorylation sites by amino acid in infected cells and normal RBCs (Fig. 1B) is similar to a previous large scale phosphorylation study in humans reporting 6600 sites [30]. We find similar distributions of phospho-sites between infected cells and normal cells for serine (79.9% vs 76.3%) and threonine (18.2% vs

17.9%) and higher tyrosine phosphorylation for normal cells with 5.8% compared to 1.8% in infected cells.

We supplemented the phosphorylation information with knowledge from additional sources about these sites and found that 17 sites have been reported in the review by Pantaleo et al. [4] about phosphorylation changes in red cell membranes of normal and diseased red cells, and that 359 sites (72.5%) are stored in the Kinexus PhosphoNET database [31] including 267 sites with experimental evidence for detection in various cell types and 92 bioinformatically predicted sites. We also compared our compendium of phosphorylation sites with results from small scale protein phosphorylation studies [4,12] by two dimensional gel electrophoresis combined with mass spectrometry in normal RBCs and *P. falciparum* trophozoite-infected RBCs. Wu et al. [12] reported 34 human protein phosphorylation sites of which 25 are present in our compendium, and Pantaleo et al. [4] identified 22 phospho-sites during parasite growth including 3 reported here. Finally, we added gene ontology cellular localisation annotation to highlight phosphorylation sites in the red cell cytoskeleton. In total we find 94 RBC cytoskeleton phospho-sites specifically detected in infected cells, and 143 specific sites in the membrane of normal RBCs.

3.2. Phosphorylation motif analysis

Our compendium of 495 phosphorylation sites detected in normal and *P. falciparum*-infected red blood cells enabled us to identify shared phosphorylation motifs and to predict associated protein kinase activity in red cells. Firstly, we compared phosphorylation motif classes between infected and normal red cells (Fig. 1C), with motif classes based on their chemical properties previously described in the schizont phosphoproteome [14]. Almost identical distributions of the acidic and proline-directed classes are found between normal and infected RBCs, whereas a 3.25-fold upregulation of basic-directed motifs and a 3-fold downregulation in tyrosine-directed motifs are observed in iRBCs. Secondly, phosphorylation sites were mapped to motifs with the phosphorylation motif finding algorithm MotifX [18], and we identified 7 phosphorylation motifs (Fig. 1D): 4 acidic-directed motifs (motif 1: [pS/pT]xx[E/D], 4: [pS/pT]x[E], 6: [pS/pT] [E/D] [E/D],[E/D], 7: [pS/pT]x[E/D][E/D]), 2 proline-directed motifs (motif 2: [pS/pT][P], 5: [R/K]xx[pS/pT][P] and 1 basic-directed motif (motif 3: [R/K]xx[pS/pT]. All these phosphorylation motifs were observed in proteins from

normal and infected red cells (Fig. 1D). Phosphorylation sites specifically detected in normal RBCs include all 7 motifs, while sites identified exclusively in infected RBCs include 5 motifs with the exceptions of motifs 6 and 7 that were not mapped on specific sites in iRBCs. Thirdly, the 7 motifs were associated with kinase target sites by PhosphoMotifFinder [20], where we consider primarily human protein kinases which have been detected in red blood cells by mass spectrometry (Table S2) [32,33]. This linked casein kinase II to 133 phosphorylation sites (motifs 1,4, 6 and 7) and protein kinase A/protein kinase C to 78 sites with motifs 3 and 5. Motif 2 [pS/pT][P] is mapped to several protein kinases (ERK1,ERK2, CDPK5 and GSK3) with 67 sites, where all four kinases have escaped detection by mass spectrometry in RBCs so far [32,33].

3.3. Functional Implications of RBC phospho-proteomes

The functional implications of the phospho-proteome to RBC physiology were assessed by GO enrichment analyses of the 123membrane associated RBC phospho-proteins compared to all human proteins using DAVID [21,22]. The enrichment results for cellular component, molecular function and biological process ontologies are depicted as a histogram plot with bars representing terms for infected and normal RBCs (Fig. 2A). The strongest signals are found for the spectrin-associated cytoskeleton with 170-fold enrichment for infected RBCs and 115-fold enrichment in normal red cells, followed by spectrin-binding with 154-fold enrichment in infected RBCs and 114-fold enrichment in normal RBCs. This trend of stronger enrichment in iRBCs than in normal RBCs is observed for all cytoskeleton-related GO terms. All GO terms functionally associated with the cytoskeleton and surface membrane of infected RBCs were organized and visualised in a network (Fig. 2B) using the Cytoscape plugin Enrichment Map [23], where each term is represented by a node with edges showing degree of overlap between GO term sets. The cytoskeleton subnetwork of infected RBC GO terms – depicted as cluster A in Fig. 2B – is composed of 35 terms out of 43, with 8 terms specific for iRBCs and 27 terms showing higher enrichment in iRBCs.

Most terms relate to cytoskeleton organization and regulatory processes, e.g. for actin filament polymerization and protein complex assembly, and thereby highlighting associated proteins with roles in orchestrating red cell shape and deformability. The

filament proteins making up the ordered meshwork forming the cytoskeleton in red cells are observed phosphorylated in infected and normal red cells (Fig. 3A). Spectrins, actin, protein 4.1, adducin, dematin, tropomyosin and tropomodulin show multiple phosphorylation sites presumably regulating cytoskeleton organization. Several transmembrane glycoproteins with transbilayer domains (Band 3, glycophorin C) anchoring the cytoskeleton via their cytoplasmic domains are regulated by kinase activity via multiple phosphorylation sites.

The phosphorylation status in our compendium for the main erythrocyte cytoskeleton proteins, transporters and various membrane associated proteins in normal and infected RBCs is listed in Fig. 3B, which shows that *P. falciparum* infection likely induces specific changes in RBC phosphorylation status. For the cytoskeleton protein 4.2, spectrin alpha chain, the glucose transporter 1 (GLUT-1), and for membrane associated proteins we observe strong upregulation of *P. falciparum* induced sites with the detection of more than 50% specific sites.

3.4. Wet-bench validation of some phospho-sites and their cAMP dependence

Given that infection of RBC by *P. falciparum* leads to a rise in intra-erythrocyte cAMP levels [34–37] combined with our identification of two potential PKA phosphorylation motifs we decided to ask how many of the phospho-sites detected in infected erythrocyte proteins are phosphorylated by a cAMP-dependent kinase. To this end, we compared the phosphorylation status of red blood cell adducin, dematin, Band 3 and GLUT-1 in uninfected RBC stimulated or not by cAMP-stimulation to their phosphorylation status in iRBC (Fig. 4). With adducin we focussed on two phospho-sites; namely, Ser59 and Ser726 and for dematin we examined Ser403, as for both proteins antibodies against these specific phospho-sites are commercially available (Fig. 4A). Phosphorylation of Ser59 in adducin can be observed in uninfected ghost lysates (lane 1), where the degree of phosphorylation increases following cAMP-stimulation (lane 2) and is completely ablated by phosphatase treatment (lane 3). Thus, Ser59 is a bona fide cAMP-dependent kinase site. Ser59 is also observed in iRBC ghost lysates and the phospho-signal is ablated by phosphatase treatment (lane 5). However, comparing lanes 1 and 4 leads to the conclusion that - although Ser59 is a cAMP dependent site - the level of phosphorylation in iRBC is similar to non-infected erythrocytes i.e. infection doesn't appear to increase phosphorylation of

Ser59. By contrast, Ser726 of adducin is phosphorylated only in iRBC, and in non-infected erythrocytes phosphorylation of Ser726 is not sensitive to cAMP stimulation (compare lanes 2 and 4). Phosphorylation of Ser726 in iRBC is ablated by phosphatase treatment, but this site does not appear to be a substrate for a cAMP-dependent kinase. Ser726 occurs within a motif 3 context (Fig. 1D) that was ambiguously mapped to PKA or PKC and the data in Fig. 4A suggests that in infected RBC it is PKC rather than PKA that phosphorylates Ser726 of adducin.

Ser403 in dematin can be observed weakly phosphorylated in erythrocyte ghost lysates (lane 1) and its phospho-status increases under the influence of cAMP (lane 2) and is significantly diminished by phosphatase treatment (lane 3). In infected erythrocytes one can observe a strong band that is insensitive to phosphatase treatment (lanes 4 and 5) indicating a likely non-specific cross-reactivity of the pSer403 antibody to an unknown parasite protein present in the iRBC ghost preparation.

The apparent lower molecular weights of 48 and 52 kDa dematin isoforms following phosphatase treatment of iRBCs sample (Fig. 4A; lane 5 lower panel) suggest that dematin phosphorylation is maintained at other phosphorylatable residues during *P. falciparum* infection.

We next turned our attention to Band 3 and GLUT-1 to which there are no available phospho-specific serine or threonine antibodies, so we exploited the availability of commercial antibodies to sites phosphorylated in the context of an RxxS*/T* motif. We recall that the RxxS*/T* motif is present in cAMP-dependent PKA motif following our analysis of RBC proteins detected phosphorylated in vivo (Fig. 1D). First, the levels of both Band 3 and GLUT-1 were determined for RBC (lane 1), RBC stimulated by cAMP (lane 2) and for iRBC (lane 3). We note the drastic reduction in GLUT-1 levels observed in iRBC (lane 3) and that GLUT-1 appears highly glycosylated as judged by the smear-like signal (lanes 1 and 2). Both α-adducin and dematin levels were used as a loading control (input). Following immunoprecipitation with the sepharose-linked anti-RxxS*/T* antibody the amounts of Band 3 and GLUT-1 in the precipitate were estimated by Western blot (top two panels; IP anti-RxxS*/T*). Band 3 is readily detected phosphorylated at an RxxS*/T* site in iRBC (lane 3) and weakly detected in non-infected erythrocytes (lane 1). However, the

phosphorylation level is not increased following cAMP stimulation (lane 2) indicating that the strong signal observed following infection (lane 3) is likely to be due to erythrocyte PKC that like PKA can phosphorylate residues in the context of the RxxS*/T* motif.

The low levels of GLUT-1 observed by Western Blot for iRBC (input, lane 3) and the observed smeared signal that has been reported to be the result of protein glycosylation [38] lead us to estimate the amount of GLUT-1 present in our ghost preparations by mass spectrometry analysis of digested protein samples using label free quantification LFQ [39] (Fig. 3C). Here, glycosylation does not interfere with the quantification measurement and similar GLUT-1 relative protein abundances were determined in infected and normal RBCs, which was expected due to the high levels of glucose consumption by iRBC [40]. After immunoprecipitation with anti-RxxS*/T*, however, the signal in iRBCs (lane 3) appears stronger than in non-infected cells, stimulated or not by cAMP (lane 1 and 2). As for Band 3, this suggests an increase in GLUT-1 phosphorylation for this motif upon infection.

4. Discussion

In this study we used a comparative analysis of phosphorylation sites between normal and *P. falciparum*-infected red blood cells and showed that the main host proteins determining cell shape, rigidity/ deformability or permeability are differentially phosphorylated/dephosphorylated upon infection. The compendium of human sites was compiled from published phospho-proteome studies generated by liquid chromatography tandem mass spectrometry focussed at the schizont life cycle stage during asexual development in RBCs. These sites were reported in supplementary tables as ‘by-products’ to *P. falciparum* phosphorylation sites without further functional interpretation and have gone largely unnoticed.

Our phosphorylation analysis is quite stringent, as it required that a given phospho-site be detected in at least 2 independent studies done in separate laboratories. This identified 495 sites in 182 human RBC proteins of which 379 sites in 153 proteins can be detected in normal RBC, and 274 sites (91 proteins) detected in iRBC of which 158 in 57 proteins are in common. This indicates that 116 sites belonging to 50 proteins appear to be specifically phosphorylated upon *P. falciparum* infection, and that 221 sites belonging to 113 proteins are likely be subjected to phosphatase

activities in iRBCs. Strikingly, in iRBCs tyrosine phosphorylation appears less frequent (5.8% down to 1.8%) suggesting that infection has induced tyrosine phosphatase activity. The parasite lacks any gene encoding classical tyrosine kinases [41] and consequently, all tyrosine phosphorylation events in erythrocyte and parasite proteins likely derive from erythrocyte tyrosine kinase activity. We consider the alternative explanation of incorrect phosphorylation localisation in normal RBCs less likely than increased phosphatase activity in iRBCs given that 62.5% of the sites have been confirmed experimentally, or predicted [31]. Amongst the 22 pY sites in normal RBCs we find a site in a protein phosphatase (PTPRD_HUMAN Y274) potentially involved in switching on phosphatase activity in infected RBCs. Other candidate tyrosine phosphatases in red cells are ACP1 and PTPRC (CD45) that have been detected in red cells by mass spectrometry [32,33] (Table S2).

Previous small scale phosphorylation studies in iRBCs of the trophozoite life cycle stage by Wu et al. [12] and Pantaleo et al. [4] analysed respectively 34 and 18 spots (Table S3) isolated from two dimensional protein gels. The majority of the sites (73.5%) detected by Wu et al. are present in our compendium that is covering the schizont asexual life cycle stage, but not the trophozoite stage, while most sites detected by Pantaleo et al. (86%) are absent in our compendium. These studies highlighted the role of protein phosphorylation in the interactions between the parasite and its human erythrocyte host and reported phosphorylation sites in key cytoskeletal proteins, e.g. spectrin beta, ankyrin 1, Band 3, alpha and beta adducin, Band 4.1, and dematin. All these proteins are found phosphorylated in our compendium, although some sites have escaped detection. Dematin pS403 is an example that has been detected by peptide NELKKKApSLF that allows for three miscleaved tryptic sites in the identification searches. In our compendium most studies utilised standard identification settings including 2 miscleavages and thereby likely excluded the identification of this peptide.

The role of protein phosphorylation in alterations of red cell membrane and cytoskeleton is evident from the GO enrichment analysis of the 123 membrane-associated RBC phosphoproteins (Fig. 2). This analysis shows that spectrin-associated cytoskeleton is 170-fold enriched in iRBC up from 114-fold in normal RBC, which supports the findings of trophozoite-infected red blood cells [4,12]. Generally, it is consistent with infection particularly inducing phosphorylation of

spectrin-associated functions like actin filament polymerization and protein complex assembly highlighting parasite-induced orchestration of red cell shape and deformability. For example, following *P. falciparum* infection more than 50% of the specifically induced sites were in protein 4.2, spectrin alpha chain and the glucose transporter GLUT-1 (Fig. 3).

We identified 7 short linear consensus sequences around phosphorylated residues determining the phosphorylation motif for protein kinase activities for 56% of the phosphorylation site compendium. The phosphorylation motifs are observed in normal and infected RBCs suggesting that human kinase activity is primarily responsible for phosphorylation events involving these sites in infected RBCs. Global proteome studies of red cells [32,33] reveal a limited repertoire of 16 human serine/threonine protein kinases (Table S2) potentially recognising these 7 phosphorylation consensus site motifs. The limited number of protein kinases detected by mass spectrometry in RBCs facilitates linking protein kinase activities with phosphorylation motifs by eliminating protein kinases that are absent in RBCs from ambiguous bioinformatics predictions. This revealed prominent roles for casein kinase II (CK2) activity in red cells with 133 predicted sites, and agrees well with the reported involvement of CK2 in phosphorylating cytoskeletal proteins (e.g. spectrin, adducin, ankyrin, and protein 4.1) [42,43], in phosphorylation of the blood group antigens Kell and Kx [44], in regulation of spectrin binding by phosphorylated ankyrin [45] and in regulating cytoadherence of *P. falciparum*-infected red blood cells [46].

Although all CK2 sites were observed in normal and infected RBCs, the 34 CK2 sites mapping to motifs 6 and 7 (Fig. 1D) are absent in the sites exclusively observed in infected RBCs. This suggests that parasite infection induces phosphatase activities that dephosphorylate CK2-positive sites to modulate red cell morphology. Protein 4.1, which is a major structural element of the red cell cytoskeleton and regulates mechanical stability, is dephosphorylated upon infection at pS104 and pS95, and ankyrin – which forms the bridge between the integral membrane protein Band 3 and spectrin – is dephosphorylated at pS817.

The motif analysis highlighted prominent roles for PKA/PKC involving 78 phosphorylation sites. For this reason, we compared the phosphorylation status of specific sites in adducin, dematin, Band 3 and GLUT-1 in uninfected RBC stimulated

or not by cAMP to their phosphorylation status in iRBC. With adducin we focussed on two phospho-sites; namely, Ser59 and Ser726 and for dematin we examined Ser403, as both proteins can be phosphorylated at these sites by cAMP-dependent PKA [47–50], and phosphosite-specific antibodies are commercially available. When we examined Ser59 of adducing in normal RBC we observed an increase in its phosphorylation status following cAMP-stimulation. We point out that cAMP-stimulation was performed using intact RBCs, right before ghost preparation. However with this caveat, *P. falciparum* infection that leads to increased cAMP levels and greater PKA activity [34–37] does not lead to a detectable increase in Ser59 phosphorylation in iRBC. By contrast, Ser726 is detected as a doublet by the phospho-specific antibody only in iRBC, but its phosphorylation in uninfected RBC isn't induced following cAMP-stimulation implying that in iRBC Ser726 phosphorylation is not by cAMP-dependent PKA, but perhaps by another host or exported parasite AGC-like kinase. There are two isoforms of dematin in normal RBC [32,33] and Ser403 phosphorylation is induced up cAMP-stimulation [47–49], but neither isoform is observed phosphorylated in iRBC, suggesting that infection has led to dephosphorylation of S403 in dematin. Surprisingly, the commercial phospho-Ser403 antibody strongly detected a signal band in iRBC that likely represents a cross-reactive parasite protein present in the ghost preparation.

As there are no specific antibodies to phosphorylated serines and threonines in Band 3 and GLUT-1 we exploited a commercial sepharose-linked antibody that reacts with residues phosphorylated in the context of RxxS*/T* that resembles closely the enriched PKA motifs (3 & 5 in Fig. 1D). Following immunoprecipitation the precipitates were probed with specific antibodies to Band 3 and GLUT-1. *P. falciparum*-infection of RBC induces phosphorylation of Band 3 at one or more RxxS*/T* sites and careful inspection of human Band 3 reveals the presence of 3 sites (RyqS*(S349); KpdS*(S356) and KasT*(T746)) all of which have been detected phosphorylated in iRBC [14,16]. However, cAMP-stimulation of normal RBC did not induce phosphorylation at any RxxS*/T* site implying that in iRBC infection-induced phosphorylation at S349, S356, or T746 is by cAMP-independent kinase.

The situation with GLUT-1 is very intriguing, as LC–MS/MS measurements showed that GLUT-1 protein levels are equal between uninfected and infected red blood cells, while phosphorylated GLUT-1 appears enriched in anti-RxxS*/T* immunoprecipitates

from iRBC (Fig. 4B). This result is consistent with the five GLUT-1 phospho-peptides detected specifically in iRBC (Fig. 3). Direct detection with anti-motif 4 (RxxS*/T*) of phosphorylated GLUT-1 by probing immunoblots of anti-GLUT-1 immunoprecipitates is difficult due to the glycosylation smear and reduced GLUT-1 signal in iRBCs.We propose that upregulation of GLUT-1 phosphorylation may be essential for the heightened glucose uptake of iRBC that fuels the parasite's energy metabolism and leads to high lactate output. Further experiments are required to investigate whether phosphorylation of GLUT-1 does indeed underpin increased glucose uptake by iRBC as inhibiting GLUT-1 kinase(s) could impact negatively on parasite growth.

5. Conclusion

In this study we generated a comprehensive compendium of protein phosphorylation sites in erythrocyte membrane proteins from normal and *P. falciparum*-infected RBCs. We demonstrated that the compendium is a new information source for exploration of phosphorylation sites involved in regulating red cell morphology and metabolite transport.

Funding

This work was supported by the Royal Society (UK) with the International Exchanges Scheme — 2013/R3 grant to E.L. and G.B. GB and SE were supported by the labex GR-Ex, reference ANR-11- LABX-0051, funded by the program “Investissements dxavenir” of the French National Research Agency, reference ANR-11-IDEX-0005-02. GL acknowledges support from ParaFrap (ANR-11-LABX-0024), INSERM and the CNRS.

References

[1] F. Roux-Dalvai, A. Gonzalez de Peredo, C. Simó, L. Guerrier, D. Bouyssié, A. Zanella, A. Citterio, O. Burlet-Schiltz, E. Boschetti, P.G. Righetti, B.Monsarrat, Extensive analysis of the cytoplasmic proteome of human erythrocytes using the peptide ligand library technology and advanced mass spectrometry, Mol. Cell. Proteomics 7 (2008) 2254–2269.

[2] S.R. Goodman, O. Daescu, D.G. Kakhniashvili, M. Zivanic, The proteomics and interactomics of human erythrocytes, Exp. Biol. Med. (Maywood) 238 (2013) 509–518.

[3] A. Pantaleo, L. De Franceschi, E. Ferru, R. Vono, F. Turrini, Current knowledge about the functional roles of phosphorylative changes of membrane proteins in normal and diseased red cells, J. Proteomics 73 (2010) 445–455.

[4] A. Pantaleo, E. Ferru, F. Carta, F. Mannu, G. Giribaldi, R. Vono, A.J. Lepedda, P. Pippia, F. Turrini, Analysis of changes in tyrosine and serine phosphorylation of red cell membrane proteins induced by *P. falciparum* growth, Proteomics 10 (2010) 3469–3479.

[5] S. Manno, Y. Takakuwa, K. Nagao, N. Mohandas, Modulation of erythrocyte membrane mechanical function by β-spectrin phosphorylation and dephosphorylation, J. Biol. Chem. 270 (1995) 5659–5665.

[6] S. Perrotta, E.M. del Giudice, A. Iolascon, M. De Vivo, D. Di Pinto, S. Cutillo, B. Nobili,Reversible erythrocyte skeleton destabilization is modulated by beta-spectrin phosphorylation in childhood leukemia, Leukemia 15 (2001) 440–444.

[7] S. Manno, Y. Takakuwa, N. Mohandas, Modulation of erythrocyte membrane mechanical function by protein 4.1 phosphorylation, J. Biol. Chem. 280 (2005) 7581–7587.

[8] E. Ferru, K. Giger, A. Pantaleo, E. Campanella, J. Grey, K. Ritchie, R. Vono, F. Turrini, P.S. Low, Regulation of membrane-cytoskeletal interactions by tyrosine phosphorylation of erythrocyte band 3, Blood 117 (2011) 5998–6006.

[9] S. Baumeister, P. Gangopadhyay, U. Repnik, K. Lingelbach, Novel insights into red blood cell physiology using parasites as tools, Eur. J. Cell Biol. 94 (2015) 332–339.

[10] K. Kirk, A.M. Lehane, Membrane transport in the malaria parasite and its host erythrocyte, Biochem. J. 457 (2014) 1–18.

[11] S. Sanyal, S. Egee, G. Bouyer, S. Perrot, I. Safeukui, E. Bischoff, P. Buffet, K.W. Deitsch, O. Mercereau-Puijalon, P.H. David, T.J. Templeton, C. Lavazec, *Plasmodium falciparum* STEVOR proteins impact erythrocyte mechanical properties, Blood 119 (2012) e1–e8.

[12] Y. Wu, M.M. Nelson, A. Quaile, D. Xia, J.M.Wastling, A. Craig, Identification of phosphorylated proteins in erythrocytes infected by the human malaria parasite *Plasmodium falciparum*, Malar. J. 8 (2009) 105.

[13] M.O. Collins, J.C. Wright, M. Jones, J.C. Rayner, J.S. Choudhary, Confident and sensitive phosphoproteomics using combinations of collision induced dissociation and electron transfer dissociation, J. Proteomics 103 (2014) 1–14.

[14] E. Lasonder, J.L. Green, G. Camarda, H. Talabani, A.A. Holder, G. Langsley, P. Alano, The *Plasmodium falciparum* schizont phosphoproteome reveals extensive phosphatidylinositol and cAMP-protein kinase A signaling, J. Proteome Res. 11 (2012) 5323–5337.

[15] L. Solyakov, J. Halbert, M.M. Alam, J.P. Semblat, D. Dorin-Semblat, L. Reininger, A.R. Bottrill, S. Mistry, A. Abdi, C. Fennell, Z. Holland, C. Demarta, Y. Bouza, A. Sicard, M.P. Nivez, S. Eschenlauer, T. Lama, D.C. Thomas, P. Sharma, S. Agarwal, S. Kern, G. Pradel, M. Graciotti, A.B. Tobin, C. Doerig, Global kinomic and phospho-proteomic analyses of the human malaria parasite *Plasmodium falciparum*, Nat. Commun. 2 (2011) 565.

[16] M. Treeck, J.L. Sanders, J.E. Elias, J.C. Boothroyd, The phosphoproteomes of *Plasmodium falciparum* and *Toxoplasma gondii* reveal unusual adaptations within and beyond the parasites' boundaries, Cell Host Microbe 10 (2011) 410–419.

[17] E.J. Soderblom, J.W. Thompson, E.A. Schwartz, E. Chiou, L.G. Dubois,M.A.Moseley, R. Zennadi, Proteomic analysis of ERK1/2-mediated human

586 sickle red blood cell membrane protein phosphorylation, Clin. Proteomics 10 (2013)
587 1.

588 [18] D. Schwartz, S.P. Gygi, An iterative statistical approach to the identification of
589 protein phosphorylation motifs from large-scale data sets, Nat. Biotechnol. 23 (2005)
590 1391–1398.

591 [19] G.E. Crooks, G. Hon, J.M. Chandonia, S.E. Brenner,WebLogo: a sequence logo
592 generator,Genome Res. 14 (2004) 1188–1190.

593 [20] R. Amanchy, B. Periaswamy, S.Mathivanan, R. Reddy, S.G. Tattikota, A.
594 Pandey, A curated compendium of phosphorylation motifs, Nat. Biotechnol. 25 (2007)
595 285–286.

596 [21] W. Huang da, B.T. Sherman, R.A. Lempicki, Systematic and integrative analysis
597 of large gene lists using DAVID bioinformatics resources, Nat. Protoc. 4 (2009) 44–
598 57.

599 [22] W. Huang da, B.T. Sherman, Q. Tan, J.R. Collins,W.G. Alvord, J. Roayaei, R.
600 Stephens, M.W. Baseler, H.C. Lane, R.A. Lempicki, The DAVID Gene Functional
601 ClassificationTool: a novel biological module-centric algorithm to functionally analyze
602 large gene lists, Genome Biol. 8 (2007) R183.

603 [23] D. Merico, R. Isserlin, G.D. Bader, Visualizing gene-set enrichment results using
604 the Cytoscape plug-in enrichment map, Methods Mol. Biol. 781 (2011) 257–277.

605 [24] A. Radfar, D. Mendez, C. Moneriz, M. Linares, P. Marin-Garcia, A. Puyet, A.
606 Diez, J.M.Bautista, Synchronous culture of *Plasmodium falcip*arum at high
607 parasitemia levels, Nat. Protoc. 4 (2009) 1899–1915.

608 [25] J.R. Wisniewski, A. Zougman, N. Nagaraj, M. Mann, Universal sample
609 preparation method for proteome analysis, Nat. Methods 6 (2009) 359–362.

610 [26] J. Rappsilber, Y. Ishihama, M. Mann, Stop and go extraction tips for matrix-
611 assisted laser desorption/ionization, nanoelectrospray, and LC/MS sample
612 pretreatment in proteomics, Anal. Chem. 75 (2003) 663–670.

613 [27] L. Zhou, J. Lyons-Rimmer, S. Ammoun, J. Muller, E. Lasonder, V. Sharma, E.
614 Ercolano, D. Hilton, I. Taiwo, M. Barczyk, C.O. Hanemann, The scaffold protein

615 KSR1, a novel therapeutic target for the treatment of merlin-deficient tumors,
616 Oncogene (2015).

617 [28] J. Cox, M. Mann, MaxQuant enables high peptide identification rates,
618 individualized p.p.b.-range mass accuracies and proteome-wide protein
619 quantification, Nat. Biotechnol. 26 (2008) 1367–1372.

620 [29] E. Lasonder, M. Treeck, M. Alam, A.B. Tobin, Insights into the *Plasmodium*
621 *falciparum* schizont phospho-proteome, Microbes Infect. 14 (2012) 811–819.

622 [30] J.V. Olsen, B. Blagoev, F. Gnad, B. Macek, C. Kumar, P. Mortensen, M. Mann,
623 Global, in vivo, and site-specific phosphorylation dynamics in signaling networks,
624 Cell 127 (2006) 635–648.

625 [31] http://www.phosphonet.ca/, PhosphoNET.

626 [32] T. Hegedus, P.M. Chaubey, G. Varady, E. Szabo, H. Saranko, L. Hofstetter, B.
627 Roschitzki, B. Stieger, B. Sarkadi, Inconsistencies in the red blood cell membrane
628 proteome analysis: generation of a database for research and diagnostic
629 applications, Database (Oxford) 2015 (2015), bav056.

630 [33] http://rbcc.hegelab.org, Red Blood Cell Collection.

631 [34] A. Dawn, S. Singh, K.R.More, F.A. Siddiqui, N. Pachikara, G. Ramdani, G.
632 Langsley, C.E. Chitnis, The central role of cAMP in regulating *Plasmodium*
633 *falciparum* merozoite invasion of human erythrocytes, PLoS Pathog. 10 (2014),
634 e1004520.

635 [35] A. Merckx, M.P. Nivez, G. Bouyer, P. Alano, G. Langsley, K. Deitsch, S. Thomas,
636 C. Doerig, S. Egee, *Plasmodium falciparum* regulatory subunit of cAMP-dependent
637 PKA and anion channel conductance, PLoS Pathog. 4 (2008), e19.

638 [36] G. Ramdani, B. Naissant, E. Thompson, F. Breil, A. Lorthiois, F. Dupuy, R.
639 Cummings, Y. Duffier, Y. Corbett, O. Mercereau-Puijalon, K. Vernick, D. Taramelli,
640 D.A. Baker, G. Langsley, C. Lavazec, cAMP-signalling regulates gametocyte-
641 infected erythrocyte deformability required for malaria parasite transmission, PLoS
642 Pathog. 11 (2015), e1004815.

643 [37] C. Syin, D. Parzy, F. Traincard, I. Boccaccio, M.B. Joshi, D.T. Lin, X.M. Yang, K.
644 Assemat, C. Doerig, G. Langsley, The H89 cAMP-dependent protein kinase inhibitor
645 blocks *Plasmodium falciparum* development in infected erythrocytes, Eur. J.
646 Biochem. 268 (2001) 4842–4849.

647 [38] J.F. Flatt, H. Guizouarn, N.M. Burton, F. Borgese, R.J. Tomlinson, R.J. Forsyth,
648 S.A.Baldwin, B.E. Levinson, P. Quittet, P. Aguilar-Martinez, J. Delaunay, G.W.
649 Stewart, L.J. Bruce, Stomatin-deficient cryohydrocytosis results from mutations in
650 SLC2A1: a novel formof GLUT1 deficiency syndrome, Blood 118 (2011) 5267–5277.

651 [39] J. Cox, M.Y. Hein, C.A. Luber, I. Paron, N. Nagaraj, M. Mann, Accurate
652 proteome-wide label-free quantification by delayed normalization and maximal
653 peptide ratio extraction,termed MaxLFQ, Mol. Cell. Proteomics 13 (2014) 2513–2526.

654 [40] M. Urscher, R. Alisch, M. Deponte, The glyoxalase system of malaria parasites
655 — implications for cell biology and general glyoxalase research, Semin. Cell Dev.
656 Biol. 22 (2011) 262–270.

657 [41] D. Miranda-Saavedra, T. Gabaldon, G.J. Barton, G. Langsley, C. Doerig, The
658 kinomes of apicomplexan parasites, Microbes Infect. 14 (2012) 796–810.

659 [42] G. Clari, V.Moret, Phosphorylation ofmembrane proteins by cytosolic casein
660 kinases in human erythrocytes. Effect of monovalent ions, 2,3-bisphosphoglycerate
661 and spermine, Mol. Cell. Biochem. 68 (1985) 181–187.

662 [43] T.Wei, M. Tao, Human erythrocyte casein kinase II: characterization and
663 phosphorylation of membrane cytoskeletal proteins, Arch. Biochem. Biophys. 307
664 (1993) 206–216.

665 [44] F. Carbonnet, C. Hattab, J.P. Cartron, O. Bertrand, Kell and Kx, two disulfide-
666 linked proteins of the human erythrocytemembrane are phosphorylated in vivo,
667 Biochem.Biophys. Res. Commun. 247 (1998) 569–575.

668 [45] S. Ghosh, F.C. Dorsey, J.V. Cox, CK2 constitutively associateswith and
669 phosphorylates chicken erythroid ankyrin and regulates its ability to bind to spectrin,
670 J. Cell Sci. 115 (2002) 4107–4115.

671 [46] R. Hora, D.J. Bridges, A. Craig, A. Sharma, Erythrocytic casein kinase II
672 regulates cytoadherence of *Plasmodium falciparum*-infected red blood cells, J. Biol.
673 Chem. 284 (2009) 6260–6269.

674 [47] L. Chen, J.W. Brown, Y.F. Mok, D.M. Hatters, C.J.McKnight, The
675 allostericmechanism induced by protein kinase A (PKA) phosphorylation of dematin
676 (band 4.9), J. Biol.Chem. 288 (2013) 8313–8320.

677 [48] L. Chen, J.W. Brown, Y.F. Mok, D.M. Hatters, C.J.McKnight, The
678 allostericmechanism induced by protein kinase A (PKA) phosphorylation of dematin
679 (band 4.9), J. Biol.Chem. 290 (2015) 17808.

680 [49] I. Koshino, N. Mohandas, Y. Takakuwa, Identification of a novel role for dematin
681 in regulating red cell membrane function by modulating spectrin–actin interaction,
682 J.Biol. Chem. 287 (2012) 35244–35250.

683 [50] Y. Matsuoka, C.A. Hughes, V. Bennett, Adducin regulation. Definition of the
684 calmodulin-binding domain and sites of phosphorylation by protein kinases A and C,
685 J. Biol. Chem. 271 (1996) 25157–25166.

686 [51] E.S. Zuccala, T.J. Satchwell, F. Angrisano, Y.H. Tan, M.C. Wilson, K.J. Heesom,
687 J. Baum, Quantitative phospho-proteomics reveals the Plasmodium merozoite
688 triggers pre-invasion host kinase modification of the red cell cytoskeleton, Sci. Rep. 6
689 (2016) 19766.

690 [52] D. Walliker, I.A. Quakyi, T.E. Wellems, T.F. McCutchan, A. Szarfman, W.T.
691 London, L.M. Corcoran, T.R. Burkot, R. Carter, Genetic analysis of the human
692 malaria parasite *Plasmodium falciparum*, Science 236 (1987) 1661–1666.

693 [53] C. Lambros, J.P. Vanderberg, Synchronization of *Plasmodium falciparum*
694 erythrocytic stages in culture, J. Parasitol. 65 (1979) 418–420.

695

Figure Legends

Fig. 1. Compendium of protein phosphorylation sites in human red blood cells

Compendium of protein phosphorylation sites in human red blood cells. A. Venn diagram depicting phospho-peptide counts in normal and P. falciparum-infected RBCs with data collected by Soderblom et al. [17] (normal RBCs) and by several independent studies of the schizont life cycle stage [13–16]. B. Distribution of amino acid phosphorylation for serine, threonine and tyrosine in phospho-proteomes. C. Pie chart showing the distribution of phosphorylation motif classes in RBC proteins for normal and infected red cells. The phosphorylated residue is located at the central position within a sequence window of 13 amino acids. Classes were defined by the chemical properties of the sequence window peptide as acidic, basic, proline-directed, tyrosine-directed or other by a decision tree method described earlier [14]. D. Table of phosphorylation motifs in normal and infected RBCs identified by Motif-X [18] analysis with phosphorylation motifs depicted as sequence logos. Putative protein kinases associated with these motifs were predicted by PhosphoMotifFinder [20].

Fig. 2. Functional annotation of red blood cell phospho-proteomes

Functional annotation of red blood cell phospho-proteomes. A. GO enrichment of membrane-associated phosphoproteins in normal and infected RBCs for the ontologies molecular function (red bars), cellular component (green bars), and biological processes (blue bars). Fold enrichment in the phospho-proteome relative to the human proteomeis displayed at the xaxis. B. Network visualisation of the overlap between enriched GO terms in infected RBCs by Cytoscape plugin Enrichment Map. Nodes represent GO terms and edges display overlap between terms with line thickness corresponding to degree of overlap. Node numbers refer to GO terms listed in the left column in A.

Fig. 3. **Phosphorylation of RBCmembrane and cytoskeleton proteins**

A. Schematic representation of a cross section from the red cell membrane shows protein phosphorylation of the key players spectrin, actin, tropomyosin and Band 4.1, which are forming a meshwork laminating the inner surface of the membrane. Linkage to the lipid bilayer membrane via ankyrin occurs with the transmembrane protein Band 3 and glycophorin C, the surface glycoprotein CD47, Rh and Rh-associated glycoprotein (RhAG) establishing the bridges with the cytoskeleton meshwork. Proteins are provided with numbers representing counts of phosphorylation sites specifically detected in infected RBCs and counts of all sites. B. Table highlighting the phosphorylation status of the main erythrocyte cytoskeleton proteins, transporters and various membrane-associated proteins in normal and infected RBCs. *Proteins with more than 50% of infected specific sites. The majority of proteins in this figure (eg glycophorin A&C, ankyrin, spectrins, adducins, band 3, dematin, protein 4.1, GLUT1, CA1&2, actin, nucleoside transporter 1) have recently been reported phosphorylated following merozoite binding to the RBC surface (Zuccala ES et al, Sci. Rep. 6:19766 [51]).

Fig. 4. **Wet-bench validation of phospho-sites and their cAMP-dependence**

A. Immunoblots showing phospho-Ser59, phospho-Ser726 and α-adducin (81 kDa), left panel; phospho-Ser403 and α and β dematin (48 and 52 kDa), right panel; using ghost lysates obtained from uninfected RBCs (lanes 1–3) and N95%-enriched schizont stage of P. falciparum (NF54)-infected RBCs (lanes 4, 5); uninfected RBCs incubated 30 min at 37 °C in the presence of 50 μM dibutyryl-cAMP (lane 2); dephosphorylated ghost lysates prepared by incubation with λ-protein phosphatase (lanes 3, 5). 1 × 107 uninfected RBCs and *P. falciparum* (NF54)-infected RBCs representing 5 μg and 30 μg total proteins, respectively. B. Immunoprecipitation/ immunoblot analysis of ghost lysates from uninfected RBCs and N95%-enriched schizont stage of *P. falciparum* (NF54)-infected RBCs (1 × 108). Immunoblots of total ghost lysates, where lane 1 = uninfected RBC; lane 2 = RBC stimulated with cAMP; lane 3 = iRBC, showing levels of Band 3 (95 kDa) and GLUT-1 (54 kDa), with α-adducin and dematin levels taken as loading controls (input). Top two panels show amounts of Band 3 and GLUT-1 immunoprecipitated by the anti-RxxS*/T* antibody (IP anti-RxxS*/T*). Note the drastically reduced Western blot signals of GLUT1

detected in total ghost lysates from iRBC (compare lanes 1, 2 with 3). The low-amount of GLUT-1 in the anti-RxxS*/T* precipitate contrasts with phospho-Band 3 that is readily detected (lane 3, top panel). C. Measurement of GLUT-1 protein abundance in isolated ghosts from infected and uninfected RBCs analysing 500 ng tryptic digests by liquid chromatography tandem mass spectrometry using label free quantification in triplicate runs. Similar GLUT-1 protein levels are observed in iRBC and RBC.

763 **Figure 1**

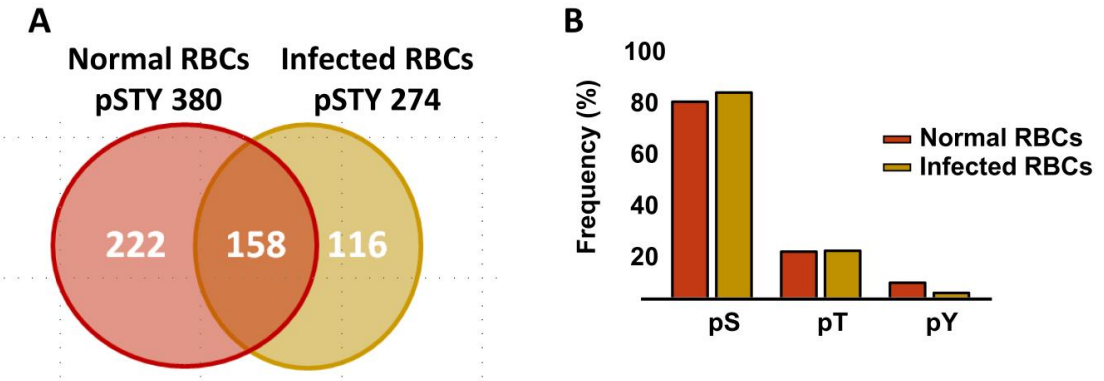

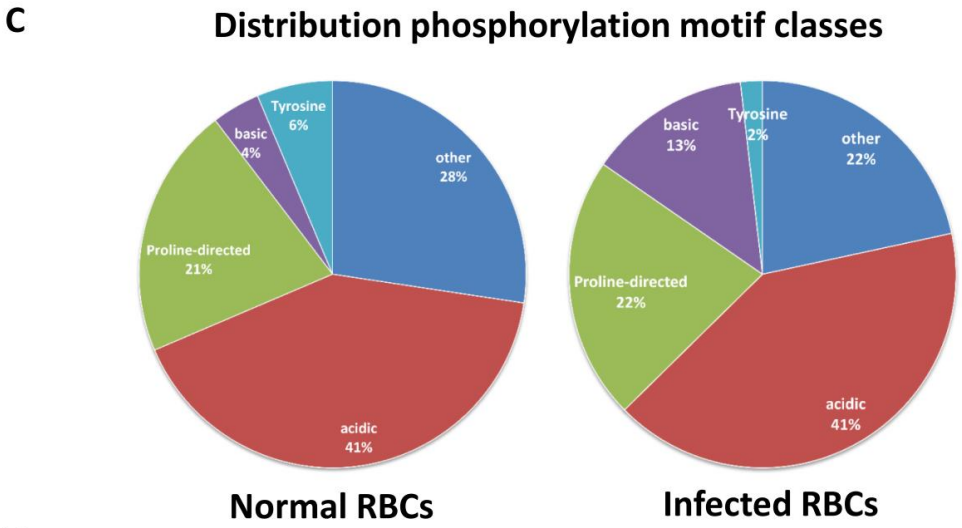

D

	Phosphorylation Motif	Protein Kinases	Shared SITES	SPECIFIC SITES Infected RBC	normal RBC
1		Casein Kinase II	30	19	23
2		Erk1, Erkw, SAPK, CDPK5, GSK3	27	15	25
3		PKA	16	14	21
4		ATM	11	8	8
5		PKA	12	6	9
6		Casein Kinase II	10	0	16
7		Casein Kinase II	3	0	5

764

765 **Figure 2**

A: Gene Ontology Enrichment

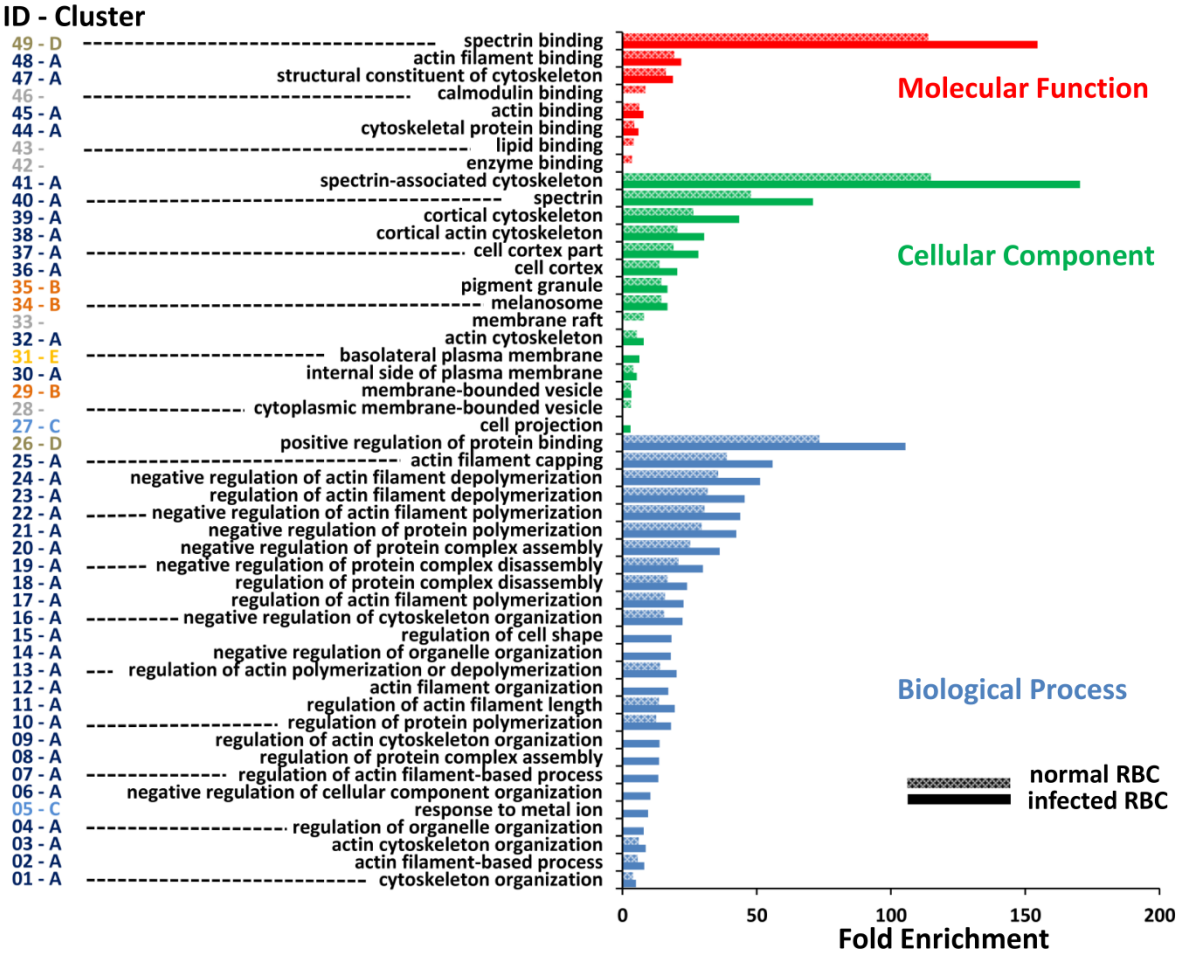

B: GO networks infected RBCs

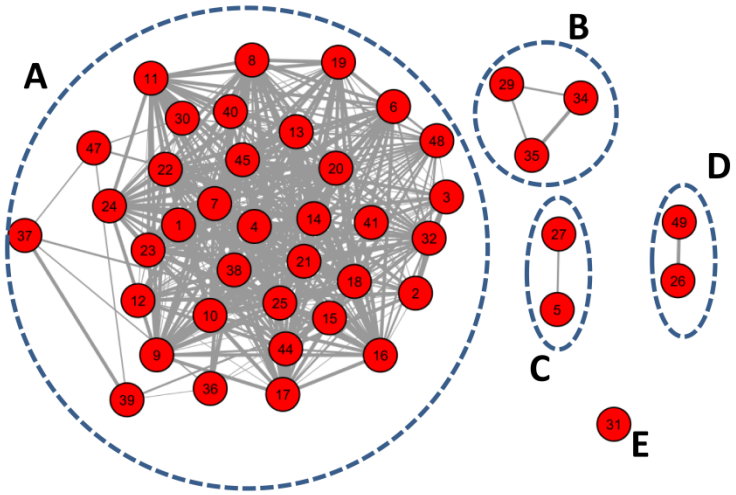

766

767

768

769 **Figure 3**

A

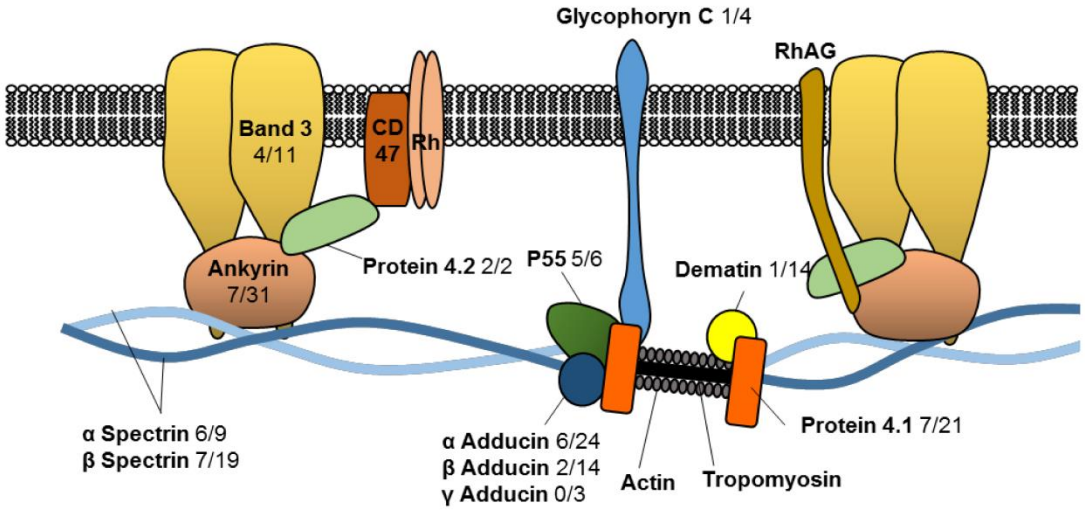

B

	Protein name	all sites	Infected RBC specific sites	RBC specific sites	Common sites
cytoskeleton	Protein 4.1	21	7	7	7
	Protein 4.2 *	2	2	0	0
	Alpha adducin	24	6	7	11
	Beta adducin	14	2	4	8
	Gamma adducin	3	0	1	2
	Ankyrin-1	31	7	3	21
	Dematin	14	1	4	9
	Spectrin alpha chain *	9	6	0	3
	Spectrin beta chain	19	7	1	11
	Stomatin	3	1	0	2
transporters	PMCA	1	0	1	0
	Aquaporin-1	3	1	0	2
	Band 3	11	4	1	6
	GLUT-1 *	7	5	0	2
	Eq.nucleoside transporter 1	5	2	0	3
Membrane - associated	Carbonic anhydrase 1 *	2	2	0	0
	Carbonic anhydrase 2 *	1	1	0	0
	CD44 antigen *	2	2	0	0
	Cytochrome b reductase 1 *	2	2	0	0
	P55 *	6	5	0	1
	GAPDH *	1	1	0	0

770

771

772

773

774

775 **Figure 4**

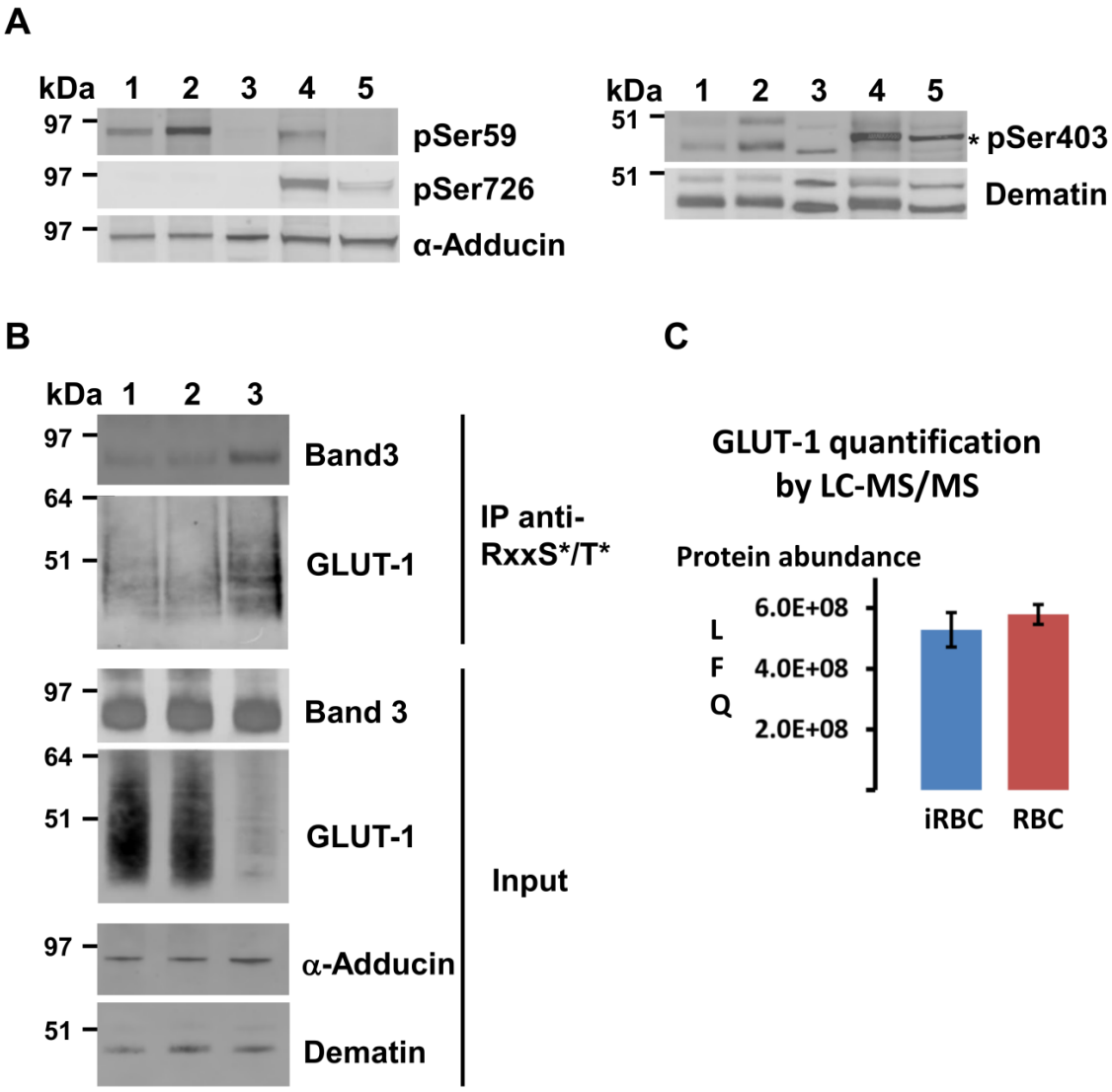

776